Water-stable blue-emitting ZnO@polymer core–shell microspheres

Huan-Ming Xiong, Dong-Ping Xie, Xiao-Yan Guan, Yu-Jing Tan and Yong-Yao Xia*

Received 5th January 2007, Accepted 21st March 2007
First published as an Advance Article on the web 2nd April 2007
DOI: 10.1039/b700176b

Two kinds of ZnO@polymer core–shell nanoparticles were prepared through polymerization initiated by the inherent free radicals on the ZnO surface. The as-prepared quantum dots exhibited intense blue fluorescence. They were used as raw materials to synthesize blue-emitting ZnO@polymer core–shell microspheres which were very stable, even in aqueous solutions of strong acids or alkalis. These microspheres, as stable aqueous suspensions, showed moderate quantum yields, and their self-assembly behavior and biomedical application could be expected.

Introduction

Photoluminescent quantum dots, especially II–VI semiconductor nanoparticles including CdS (Se, Te) and ZnO (S, Se, Te), have been the subjects of intensive research in the past 20 years.[1–11] These II–VI semiconductors can be divided into two groups according to their valence–conduction band gaps. Group I have narrow band gaps, such as CdSe (1.7 eV) and CdTe (1.5 eV). Their emission wavelengths can be tuned from green to red by controlling the particle size, and their luminescent mechanism is well known: fluorescence results from electron transition from the conduction band to the valence band. Therefore, syntheses of these nanoparticles aim at morphological uniformity, high crystallization and surface passivation. In contrast, Group II share wide band gaps, *e.g.*, ZnO (3.4 eV) and ZnS (3.6 eV). Adjusting ZnO emission wavelengths from blue to yellow has just been realized successfully.[12,13] However the visible fluorescent origination involving surface vacancy mechanisms is not very clear.[14,15] The highly crystallized ZnO nanocrystals also exhibit band gap fluorescence like those in Group I,[16,17] while the corresponding emission is located in the ultraviolet region and the quantum yield (QY) is very low.[18] Undoubtedly, the surface state of ZnO nanoparticles plays the main role that determines their visible fluorescence. However, such a luminescent mechanism related to surface vacancies, in which the trapped electrons and holes recombine randomly at various energetic levels, means that the ZnO visible emission has a rather broad peak and a quite low quantum yield.[19] Therefore, to obtain ZnO nanomaterials with intense visible luminescence, it is necessary to find suitable ways for surface modification and the photoluminescent process should not be limited within ZnO itself.

The classical sol–gel method to prepare ZnO colloids involves hydrolyzing zinc acetate by LiOH in ethanol.[20–22] The as-prepared green-emitting ZnO nanoparticles are protected by acetic groups which are covalently bonded to the ZnO surfaces. The emission band of these ZnO colloids continues to red shift slowly at room temperature and precipitation is observed after weeks, because the small acetic groups are insufficient to hinder ZnO nanoparticles from aggregation and growth. In order to protect ZnO quantum dots more effectively, we designed a new ligand which had a polyethylene glycol chain on one end and an acetic group on the other.[12] After this ligand was attached to the ZnO surface through covalent bonds, the emission wavelengths of the obtained ZnO colloids were stable for weeks. So the ZnO visible fluorescence could be tuned from blue to yellow by controlling the synthesis conditions.[13] Similarly, another ligand with an ionic liquid group on one end showed better protection because the surface charged ZnO nanoparticles repel one another.[23] However, whichever ligand is used, the coordination equilibria between ligands and nanoparticles will be inevitably destroyed by increasing temperature or changing ligand concentration.[24,25] For example, ZnO nanoparticles which are stable in water have not been reported yet. The fact is that ligand-modified ZnO nanoparticles decompose and lose fluorescence immediately when they encounter water.

Forming core–shell structures by initiating polymerization on ZnO nanocrystal surfaces seems to be the optimal choice to protect ZnO, because polymerization is irreversible and the polymer shell is so dense that ions or molecules can not penetrate to destroy the cores. Unfortunately, obtained through either dissolving initiators in monomers or grafting initiators on quantum dot surfaces, the polymerization products are often insoluble bulk materials, but no longer nano-scaled materials.[26,27] As a result, further processing or assembly for application in photonic or optoelectronic devices is restricted. So far, only a few kinds of polymer beads containing CdTe cores have been synthesized, while the synthesis conditions were complex and critical in order to prevent CdTe from quenching.[28,29] Another reasonable strategy is to utilize the inherent radicals on the ZnO surface to initiate polymerization. The direct polymerization of methyl methacrylate (MMA) using ZnO quantum dots as photoinitiators has been reported, but this process needed very strong irradiation and the product beads were so large that they precipitated from the reaction solutions.[30] Thereafter, similar experiments employing ZnO nanoparticles as initiator have not been reported.

Recently, we polymerized MMA on specially pretreated ZnO nanocrystal surfaces at 60 °C with neither irradiation nor

Department of Chemistry and Shanghai Key Laboratory of Molecular Catalysis and Innovative Materials, Fudan University, Shanghai 200433, People's Republic of China. E-mail: yyxia@fudan.edu.cn; Fax: (+86)-21-55664177

additive initiators. The precisely controlled reaction produced blue-emitting ZnO@polymer core–shell nanoparticles with a remarkable QY of 85%.[31] Exploring their potential application seemed attractive but suffered from the low yield at that time. After one year's effort, we have succeeded in preparing considerable amount of products by improving the synthesis techniques, and we also have obtained PS (polystyrene) coated ZnO nanoparticles in a similar way. In this paper, the UV-Vis and PL spectra of the as-prepared ZnO nanoparticles are studied in detail. Furthermore, using these nanoparticles as starting materials, we have synthesized luminescent ZnO@PMMA and ZnO@PS core–shell microspheres through a simple procedure. These microspheres possess moderate QYs and they are very stable in water, and even in the aqueous solutions of strong acids and alkalis.

Experimental

All reagents were of analytical grade, and the monomer methyl methacrylate (MMA) and styrene were purified by distillation under reduced pressure.

1. Preparation of ZnO–polymer core–shell nanoparticles

Methacrylic acid (MAA) was dissolved in water to get a MAA solution (15 wt%), the solution was heated to 70 °C and then reacted with ZnO powder to make zinc methacrylate. The solution of zinc methacrylate was evaporated to get solid zinc methacrylate and then further dehydrated in a vacuum oven at 80 °C for 5 hours. The anhydrous zinc methacrylate was dissolved in absolute ethanol and the solution was refluxed for about 3 hours at 80 °C. The Zn(II) concentration was measured by titration using EDTA in the NH_3–NH_4Cl buffer (pH = 10, eriochrome black T as an indicator). The as-prepared 0.1 M zinc methacrylate solution was mixed with 0.2 M LiOH ethanol solution at a molar ratio of [LiOH]/[Zn] = 3.5, and the reaction continued for one day at room temperature. Afterwards, the mixture was concentrated by a rotation evaporator at 40 °C until a precipitate appeared. The white precipitate was separated from the solution by centrifugation, and then dried in an oven at 100 °C for 3 minutes. The obtained solid was designated ZnO–MAA in which MAA groups were connected to the ZnO nanoparticles through covalent bonds.[31] The freshly prepared ZnO–MAA was dispersed in benzene or toluene by sonication firstly, and then mixed with MMA or styrene monomers. The mixture was heated under 60 °C for 20 minutes and then centrifuged to remove the unreacted solid. A significantly improved yield of the final products was achieved with the aid of benzene or toluene, and toluene did a better job than benzene. The obtained solutions exhibited strong blue fluorescence even in the sunlight. They were evaporated under vacuum to remove monomers and solvents, and the resulting gel-like solids were designated ZnO–P1 core–shell nanoparticles (made from MMA) or ZnO–P2 species (made from styrene). Tens of milligrams of products for both ZnO–P1 and ZnO–P2 can be synthesized when one gram ZnO powder is used as the starting materials. These nanoparticles were redispersed in absolute ethanol for optical measurements.

2. Preparation of ZnO–polymer core–shell microspheres

ZnO–P1 and ZnO–P2 solids were dissolved in MMA and styrene respectively for use. For comparison, the polymerization conditions were kept the same for different monomers: MMA, styrene, MMA containing ZnO–P1 and styrene containing ZnO–P2. A monomer was mixed with distilled water at a weight ratio of 1 : 8.5 at 75 °C, then $K_2S_2O_8$ initiator was added to the mixture. The weight ratio of the monomers *versus* initiator was 25 : 1. The reaction mixture was refluxed at 100 °C for 1 hour to obtain a milky suspension. The suspension was purified through dialysis in deionized water repeatedly to remove salts and unreacted monomers thoroughly. Such polymerization processes have good yields and grams of final solid products could be obtained for each preparation. It was seen that the ZnO@PMMA and ZnO@PS microspheres were blue-emitting under UV light, while the pure PMMA and PS samples exhibited no fluorescence.

3. Characterization

A JEM-3010 transmission electron microscope operating at 300 kV was employed to obtain HRTEM images. The PL spectra and UV-Vis absorption data were recorded on a Varian Cary Eclipse fluorescence spectrophotometer and a Perkin Elmer Lambda 40 UV-Vis spectrometer respectively. The quantum yield for each sample was calculated using quinine sulfate in 0.5 M sulfuric acid aqueous solution as the reference. A Philips XL30 scanning electronic microscope was used to obtain SEM images. The microsphere suspensions were dropped onto mica substrates and dried before atomic force microscopic (AFM) measurements on a Veeco Instrument Nanoscope IIIa microscope using a tapping mode in air. The PL photos for microsphere suspensions under UV light irradiation were taken using an Olympus BX51 fluorescence microscope.

Results and discussion

Schemes 1 and 2 describe the polymerization processes in which ZnO–MAA nanoparticles react with MMA and styrene monomers to produce ZnO–P1 and ZnO–P2 core–shell nanoparticles respectively. After the ZnO–MAA nanoparticles were freshly prepared, they were mixed with benzene or toluene immediately and then MMA or styrene monomers were added into the reaction system. Under strong sonication, the inherent free radicals on the ZnO surface probably transferred to the double bond of MAA groups to form carbon radicals which reacted with the MMA or styrene monomers. Such polymerization would continue during heating treatment until the polymer shell formed on the ZnO surface. Since the polymerization has taken place on each ZnO nanoparticle (those unreacted ZnO nanoparticles will agglomerate and precipitate when heated), almost no aggregate is observed for the final ZnO@polymer products under HRTEM as shown in Fig. 1. The average diameter of ZnO–P1 is about 2.1 nm while that of ZnO–P2 is about 2.3 nm. The polymer shells coated on the ZnO surface cannot be observed under HRTEM, but they render these ZnO nanoparticles soluble in many organic solvents, such as ethanol, chloroform,

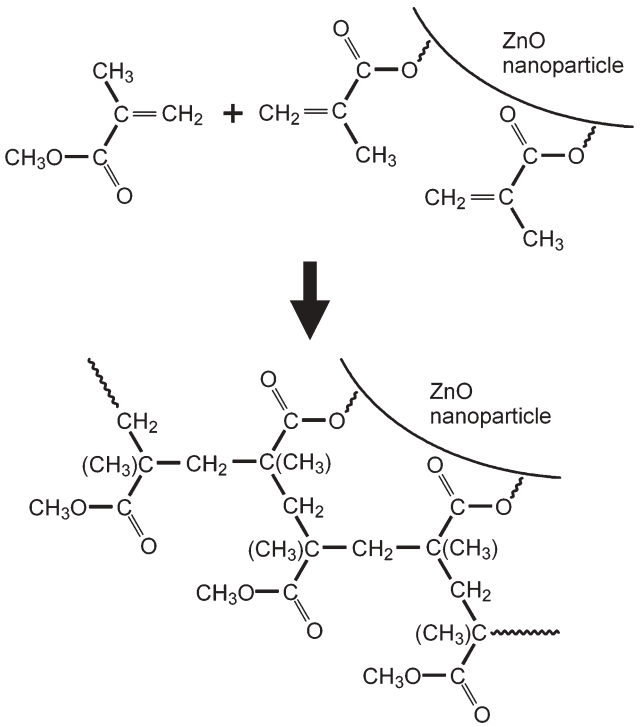

Scheme 1 Conceptual diagram illustrating the polymerization reaction MMA + ZnO–MAA → ZnO–P1.

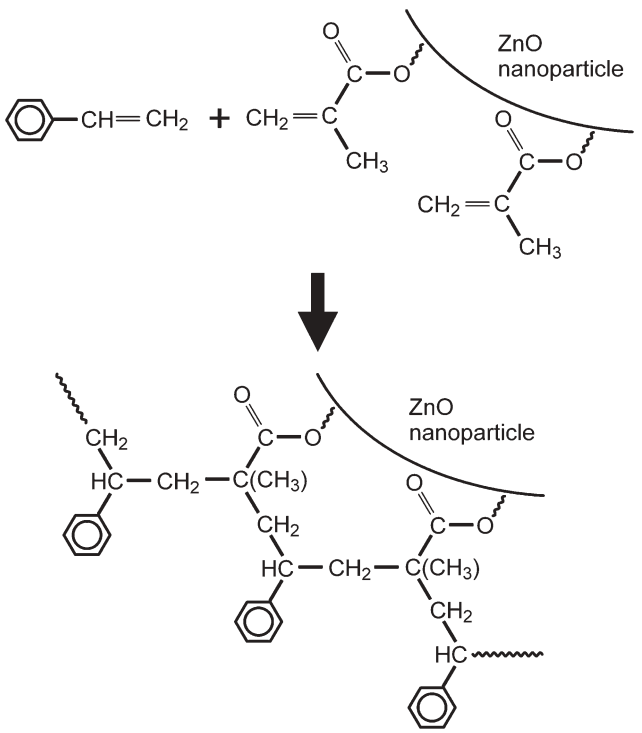

Scheme 2 Conceptual diagram illustrating the polymerization reaction styrene + ZnO–MAA → ZnO–P2.

tetrahydrofuran and benzene, indicating that this type of luminescent quantum dots can be used conveniently.

In Fig. 2, the UV-Vis absorption spectra and photoluminescent (PL) spectra of the ZnO–MAA, ZnO–P1 and ZnO–P2

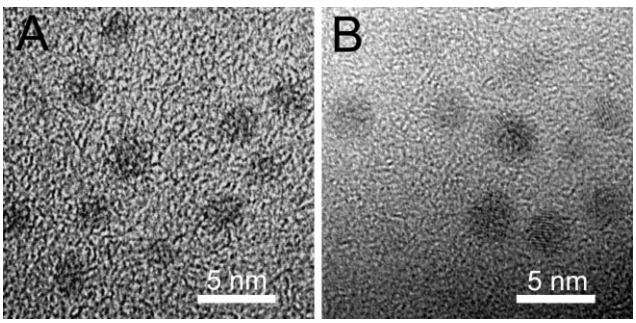

Fig. 1 HRTEM images for (A) ZnO–P1 and (B) ZnO–P2 core–shell nanoparticles.

ethanol colloids are listed for comparison. For the conventional ZnO–MAA nanoparticles, both the absorption onset and the excitation peak are at 3.77 eV while the blue emission is around 2.67 eV. This blue emission has a quantum yield of about 20% when the sample is freshly prepared. However, after the ZnO nanoparticles are coated with the polymer shells, the UV-Vis absorption and PL spectra change dramatically. The UV-Vis absorption of ZnO–P1 involves two bands. One is the typical ZnO absorption with its onset still at 3.77 eV. The other band including three peaks at 3.59, 3.45 and 3.27 eV, is ascribed to the polymer shell because the UV-Vis spectra of the polymer shell also exhibits these three peaks after the ZnO component is removed by concentrated HCl.[31] The excitation spectrum of ZnO–P1 also has three maxima at the same positions, but that corresponding to ZnO absorption is not seen, indicating that the strong blue emission at 2.95 eV results from the polymer absorption rather than from ZnO absorption. As for ZnO–P2 nanoparticles, only the polymer absorption can be observed in the UV-Vis spectra because the residual styrene or styrene oligomers have such strong absorption above 4 eV that the ZnO signals are overshadowed. Similar to ZnO–P1, the UV-Vis absorption and excitation spectra of ZnO–P2 have the same two maxima at 3.39 and 3.22 eV respectively. Since ZnO–P1 and ZnO–P2 core–shell nanoparticles have different polymer structures, differences between their absorption and excitation spectra can be expected. However, their emission spectra are almost the same, with only one peak at about 2.9 eV. According to the Levshin rule and the Franck–Condon theory,[32] there lies a mirror symmetry between the excitation spectra and the corresponding emission curve for organic molecules, *i.e.*, the ZnO–P1 emission band should possess three peaks while the ZnO–P2 emission curve should have two maxima if the blue emission originates from the organic species. Moreover, such emission cannot be regarded as the band gap fluorescence definitely, because the valence–conduction band gap of ZnO is 3.37 eV at room temperature.[33] Therefore, we believe that the strong blue luminescence arises from the ZnO nanoparticle surface.

The mechanism for ZnO visible fluorescence remains a controversial and unclear issue in the literature.[14,15] It has been agreed by researchers that the green emission arises from electrons or holes trapped on ZnO surface vacancies,[19–23] but the energetic position of the trapped carriers is difficult to determine. Hence, there are at least two possibilities involved

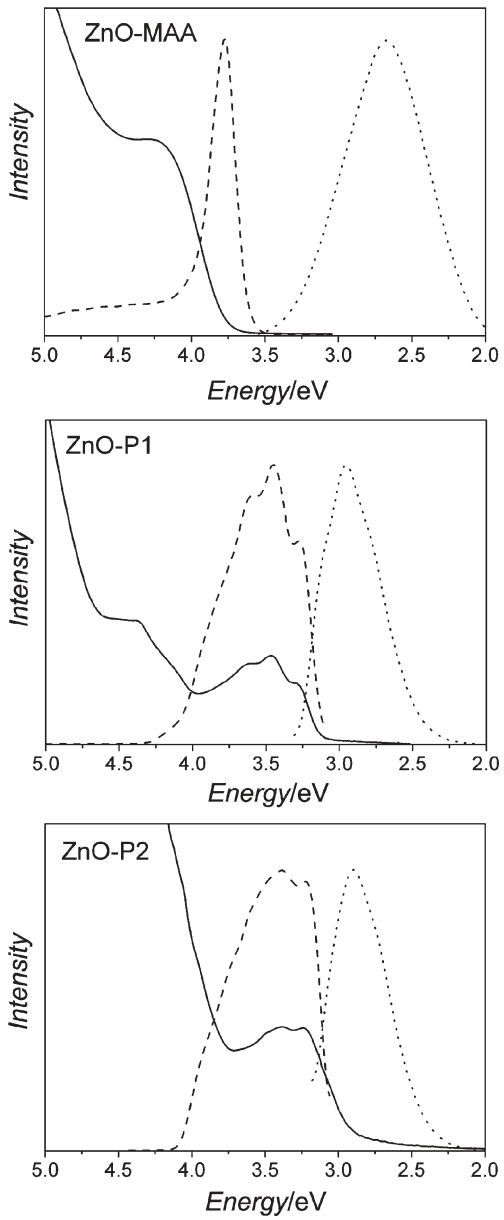

Fig. 2 UV-Vis absorption (solid lines), excitation spectra (dashed lines) and emission curves (dotted lines) for ZnO–MAA, ZnO–P1 and ZnO–P2 ethanol colloids. The excitation wavelengths for these three samples are 328, 359 and 366 nm respectively, while the excitation spectra are recorded using emission wavelengths of 464, 420 and 425 nm.

in the mechanism of ZnO visible luminescence. One is recombination of a delocalized electron with a deeply trapped hole,[14,34] while the other is recombination of a delocalized hole with a deeply trapped electron.[35,36] In our opinion, the former one is more persuasive in explaining the experimental results. However, this mechanism only concerns the green-yellow emission (500–600 nm) for ZnO nanoparticles, while the origin of the most lately found blue emission (440–460 nm) is rarely investigated. Kahn *et al.*[37] ascribed such blue fluorescence to be a transition of an electron from a level close to the conduction band edge to a shallowly trapped hole in a ZnO surface vacancy whose energetic position was a little higher than the ZnO valence band edge. Since both the photogenerated electron and the trapped hole were not deeply captured by the vacancies, their recombination was much more rapid and exhibited higher efficiency than that of those deeply trapped electron–hole couples which emitted green-yellow fluorescence. Most recently, Quist *et al.*[38] proved that the photogenerated electrons could transfer from the lowest unoccupied molecular orbital (LUMO) of the conjugated polymers to the conduction band of ZnO nanoparticles. On the basis of the above-mentioned researches and our experimental results, we suppose that in our ZnO@polymer core–shell nanoparticles the photogenerated electrons transfer from the excited state of polymer shells to the conduction band of ZnO nanoparticles, and then combine with those shallowly trapped holes in ZnO surface vacancies (as shown in Scheme 3). These holes may be captured from the polymer shell by the vacancies on the ZnO surface. If this hypothesis is true, the drawbacks of ZnO visible emission can be overcome through modifying the ZnO nanoparticle surface properly, and thus, ZnO quantum dots would replace CdSe/CdTe counterparts in practice because ZnO is cheap and nonpoisonous.

Exploring the potential applications of ZnO nanomaterials has the same importance as disclosing their luminescent mechanism. It is well known that the sulfide, selenide and telluride quantum dots can be readily prepared in aqueous solutions using organic ligands.[1–10] In contrast, investigations on luminescent ZnO colloids are usually limited to non-aqueous systems.[11–23] Incorporation of a small amount of water causes ZnO particles to grow large and lose fluorescence.[39] Such instability of ZnO quantum dots in water is due to their surface luminescent mechanisms. Water molecules are able to attack the luminescent centers on the ZnO nanoparticle surface and destroy them rapidly, and thus, the applications of ZnO quantum dots in aqueous solution, such as self-assembly and biomedical labeling, are heavily hindered. Hung and Whang[27] tried to polymerize hydrophilic hydroxyethyl methacrylate monomers around ZnO nanoparticles, but the final products were insoluble solids. Yang *et al.*[29] prepared PS beads containing CdTe cores which could be suspended in water, but the synthesis conditions were critical and complex because CdTe quantum dots were apt to be oxidized and destroyed. In contrast, our ZnO@polymer core–shell nanoparticles were very stable and miscible in monomers, so the polymerization processes to prepare ZnO@PMMA and

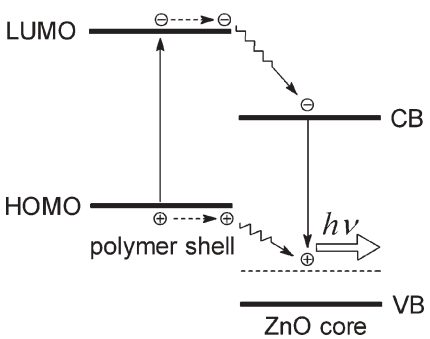

Scheme 3 Conceptual diagram illustrating the luminescent mechanism for ZnO@polymer nanoparticles.

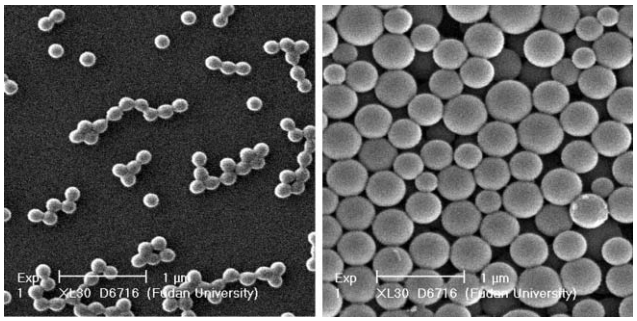

Fig. 3 SEM images of ZnO@PMMA microspheres (left) and ZnO@PS microspheres (right). The bars in both images represent one micrometer.

ZnO@PS microspheres were carried out conveniently under simple conditions.

ZnO–P1 and ZnO–P2 nanoparticles were dissolved into MMA and styrene monomers respectively, and then these monomers were polymerized to be milky suspensions in boiling water using typical $K_2S_2O_8$ initiator. For comparison, pure PMMA and PS microspheres were also synthesized under the same conditions. The obtained PMMA, PS, ZnO@PMMA and ZnO@PS microspheres were investigated by SEM, AFM and fluorescence microscopy. It was found that most microspheres were monodispersed, and the incorporation of ZnO cores had little influence on the size of both PMMA and PS species. The SEM images illustrate that the average diameter of ZnO@PMMA microspheres is about 150 nm while that of ZnO@PS species is about 450 nm, as shown in Fig. 3. However, the particle sizes resulting from AFM measurements look a little larger, which is ascribed to the measurement errors of the tapping mode. In Fig. 4, both the AFM topographs and phase images of PMMA and ZnO@PMMA are compared.

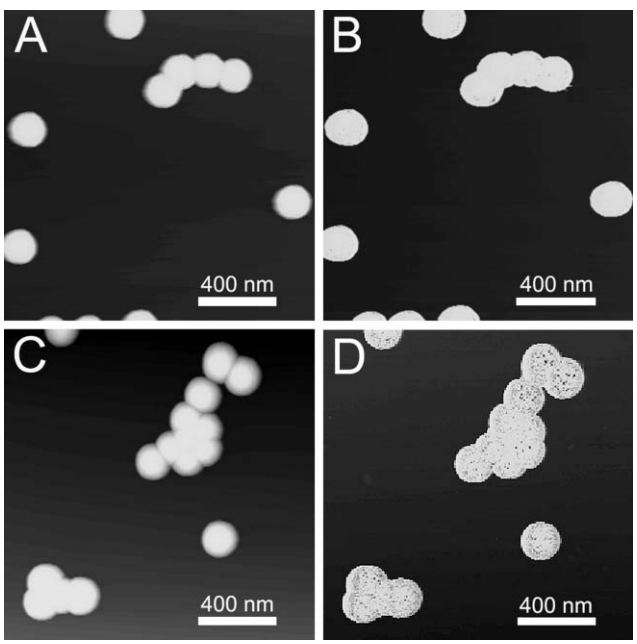

Fig. 4 AFM topographs and phase images of (A, B) the PMMA microspheres and (C, D) the ZnO@PMMA core–shell microspheres.

The microspheres appear blurry in the topographs (Fig. 4 A and C) because the polymer shells are so soft that the probe tapping causes microsphere distortion. It is fascinating that the phase image of ZnO@PMMA (Fig. 4 D) is quite different from that of PMMA (Fig. 4 B). Many dark spots are observed in the ZnO@PMMA spheres, while the colors of PMMA spheres are even. We deem that these dark spots result from phasic differences[40] between the soft polymer shells and the hard ZnO cores. Hence, the AFM data adequately prove the core–shell structure of the ZnO@polymer microspheres. It is worth mentioning that such direct observation on nanoparticle-polymer core–shell structures by the AFM technique is scarcely seen in the literature. Actually, in order to distinguish the phasic differences between ZnO cores and PMMA shells, the AFM measurement should be carried out very carefully and slowly, even lasting 24 hours for one sample.

The polymer shells protect the ZnO nanoparticles much more effectively than the conventional acetate ligands. For example, acetic group protected ZnO nanoparticles will precipitate from colloids when heated at 80 °C while our ZnO–P1 colloids maintain 60% QY after refluxing in ethanol for 10 days.[31] More surprisingly, the present ZnO@PMMA and ZnO@PS suspensions after refluxing at 100 °C in water were still able to emit blue fluorescence under UV light. Fig. 5 shows the ZnO@PMMA and ZnO@PS images recorded by a fluorescence microscope. It is obvious that the luminescent microspheres are monodispersed and the brightness of each microsphere is even, indicating that ZnO cores are dispersed homogeneously in the microspheres. In order to test the stability of the microspheres in aqueous solutions, a small amount of ZnO@PMMA sample was dispersed in water, 0.1 M HCl and 0.1 M NaOH aqueous solutions in daylight. Afterwards, the PL spectra for these suspensions were recorded every other day. The PL emission maxima *versus* storage time are shown in Fig. 6. It is found that the microspheres in both deionized water and HCl solution are very stable, while NaOH reduces the PL intensity of the ZnO@PMMA sample to some degree in the first hour, suggesting that strong alkali quenches some of the ZnO@PMMA microspheres while the surviving ones still remain luminescent in NaOH aqueous solution. The ultra-stability of the present core–shell microspheres in aqueous solutions greatly facilitates their future applications in biomedical labeling[41] and protein adsorption.[42]

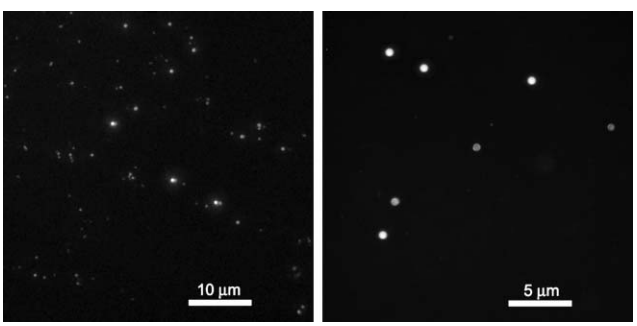

Fig. 5 PL microscope photographs of ZnO@PMMA (left) and ZnO@PS (right) microspheres excited by 365 nm UV light.

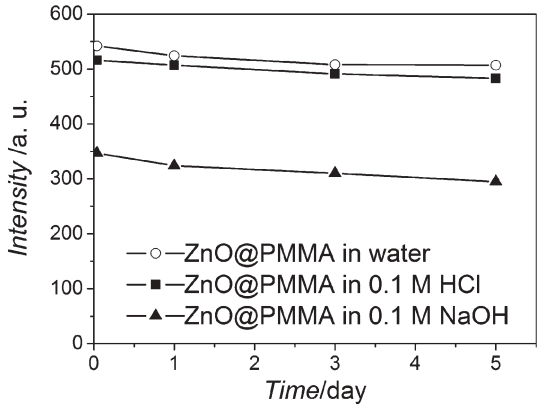

Fig. 6 Stability of PL emission intensity for ZnO@PMMA microspheres in aqueous solutions.

Although luminescent polymer–nanoparticle composites have been investigated widely, few researchers reported the quantum yields of the polymerized bulk materials. The fact is that these bulk composites exhibit much lower luminescent efficiency than the parent quantum dots. Yang *et al.*[29] reported 8–17% PL efficiency of PS beads containing CdTe cores, but the data were estimated by using a CdTe parent solution with the same concentration as the reference. Actually, in a typical procedure of QY estimation, the sample and the standard should be irradiated by the same excitation light, and at the light wavelength both the sample and the standard should have similar optical density.[7] Then the integrated emissions of both PL spectra are compared to calculate the QY of the sample, taking into account the QY value of the standard. In our experiments, quinine sulfate in 0.5 M H_2SO_4 aqueous solution was employed as the standard (QY = 55%),[19,23,27] and both the ZnO@polymer nanoparticle ethanol colloids and microsphere water suspensions are measured using the same reference. The estimated QYs for ZnO–P1, ZnO–P2, ZnO@PMMA and ZnO@PS samples are 85%, 31%, 22% and 9% respectively. The QY difference between ZnO–P1 and ZnO–P2 is due to the two distinct polymer structures, while the significant contrast between parent nanoparticles and derivative microspheres can be ascribed to two main reasons. One is chemical quenching effects during the preparation of the microspheres, including water and oxidant attack. The other is physical influences, such as UV-Vis absorption of polymer shells, re-absorption among aggregated ZnO nanoparticles inside each microsphere, diffraction caused by the microspheres with diameters close to light wavelength, and holophotal phenomena on the interface between polymer and water. Nevertheless, the ZnO@PMMA microspheres exhibit moderate efficiency in water and such blue fluorescence is unavailable as far as CdSe/CdTe species are concerned, so their future applications can be expected optimistically.

Conclusion

ZnO–P1 and ZnO–P2 core–shell nanoparticles were synthesized through polymerization initiated by virtue of the inherent radicals on freshly prepared ZnO nanoparticles. These core–shell nanoparticles exhibited strong blue emission and high quantum yields. They were further used to prepare ZnO@PMMA and ZnO@PS microsphere suspensions. Due to the effective protection by the polymer shell, the as-prepared microspheres were stable even in aqueous solutions of HCl and NaOH. Their aqueous suspensions showed moderate quantum yields, suggesting their potential use as biomedical labels and photonic crystals. Our work paves a promising path to practical applications of luminescent ZnO nanomaterials in aqueous circumstances.

Acknowledgements

This work was financially supported by the National Natural Science Foundation of China (Grant No. 20503007), 863 Project of China (No. 2006AA02Z134) and Shanghai Natural Science Foundation (Grant No. 05ZR14016).

References

1 A. P. Alivisatos, *Science*, 1996, **271**, 933.
2 S. Empedocles and M. Bawendi, *Acc. Chem. Res.*, 1999, **32**, 389.
3 X. Peng, U. Manna, W. Yang, J. Wickham, E. Scher, A. Kadavanich and A. P. Alivisatos, *Nature*, 2000, **404**, 59.
4 Z. Tang, N. A. Kotov and M. Giersig, *Science*, 2002, **297**, 237.
5 M. Han, X. Gao, J. Z. Su and S. Nie, *Nat. Biotechnol.*, 2001, **19**, 631.
6 D. V. Talapin, A. L. Rogach, E. V. Shevchenko, A. Kornowski, M. Haase and H. Weller, *J. Am. Chem. Soc.*, 2002, **124**, 5782.
7 L. Qu and X. Peng, *J. Am. Chem. Soc.*, 2002, **124**, 2049.
8 N. S. Pesika, K. J. Stebe and P. C. Searson, *Adv. Mater.*, 2003, **15**, 1289.
9 N. Pradhan, D. M. Battaglia, Y. Liu and X. Peng, *Nano Lett.*, 2007, **7**, 312.
10 H. Zhang, D. Wang, B. Yang and H. Möhwald, *J. Am. Chem. Soc.*, 2006, **128**, 10171.
11 Y. Chen, M. Kim, G. Lian, M. B. Johnson and X. Peng, *J. Am. Chem. Soc.*, 2005, **127**, 13331.
12 H. M. Xiong, D. P. Liu, Y. Y. Xia and J. S. Chen, *Chem. Mater.*, 2005, **17**, 3062.
13 H. M. Xiong, Z. D. Wang, D. P. Liu, J. S. Chen, Y. G. Wang and Y. Y. Xia, *Adv. Funct. Mater.*, 2005, **15**, 1751.
14 A. van Dijken, E. A. Meulenkamp, D. Vanmaekelbergh and A. Meijerink, *J. Lumin.*, 2000, **90**, 123.
15 *Phosphor Handbook*, ed. S. Shionoya and W. M. Yen, CRC Press, Boca Raton, FL, 1999, p. 255.
16 S. -H. Choi, E. -G. Kim, J. Park, K. An, N. Lee, S. C. Kim and T. Hyeon, *J. Phys. Chem. B*, 2005, **109**, 14792.
17 T. Andelman, Y. Gong, M. Polking, M. Yin, I. Kuskovsky, G. Neumark and S. O'Brien, *J. Phys. Chem. B*, 2005, **109**, 14314.
18 N. S. Norberg and D. R. Gamelin, *J. Phys. Chem. B*, 2005, **109**, 20810.
19 D. W. Bahnemann, C. Kromann and M. R. Hoffmann, *J. Phys. Chem.*, 1987, **91**, 3789.
20 L. Spanhel and M. A. Anderson, *J. Am. Chem. Soc.*, 1991, **113**, 2826.
21 E. A. Meulenkamp, *J. Phys. Chem. B*, 1998, **102**, 5566.
22 H. M. Xiong, X. Zhao and J. S. Chen, *J. Phys. Chem. B*, 2001, **105**, 10169.
23 D. P. Liu, G. D. Li, Y. Su and J. S. Chen, *Angew. Chem., Int. Ed.*, 2006, **45**, 7370.
24 J. Aldana, N. Lavelle, Y. Wang and X. Peng, *J. Am. Chem. Soc.*, 2005, **127**, 2496.
25 D. V. Talapin, A. L. Rogach, M. Haase and H. Weller, *J. Phys. Chem. B*, 2001, **105**, 12278.
26 H. Zhang, C. Wang, M. Li, X. Ji, J. Zhang and B. Yang, *Chem. Mater.*, 2005, **17**, 4783.
27 C. H. Hung and W. T. Whang, *J. Mater. Chem.*, 2005, **15**, 267.
28 Y. Gong, M. Gao, D. Wang and H. Möhwald, *Chem. Mater.*, 2005, **17**, 2648.
29 Y. Yang, Z. Wen, Y. Dong and M. Gao, *Small*, 2006, **2**, 898.

30 A. J. Hoffman, H. Yee, G. Mills and M. R. Hoffmann, *J. Phys. Chem. B*, 1992, **96**, 5540.
31 H. M. Xiong, Z. D. Wang and Y. Y. Xia, *Adv. Mater.*, 2006, **18**, 748.
32 *Luminescence of Molecules and Crystals*, ed. M. D. Salanin and V. Riecansky, Cambridge International Science Publishing, Cambridge, UK, 1995, pp. 53 and 128.
33 B. K. Meyer, H. Alves, D. M. Hofmann, W. Kriegseis, D. Forster, F. Bertram, J. Christen, A. Hoffmann, M. Straßburg, M. Dworzak, U. Haboeck and A. V. Rodina, *Phys. Status Solidi B*, 2004, **241**, 231.
34 A. van Dijken, E. A. Meulenkamp, D. Vanmaekelbergh and A. Meijerink, *J. Phys. Chem. B*, 2000, **104**, 1715.
35 K. Vanheusden, W. L. Warren, J. A. Voigt, C. H. Seager and D. R. Tallant, *Appl. Phys. Lett.*, 1995, **67**, 1280.
36 K. Vanheusden, W. L. Warren, C. H. Seager, D. R. Tallant, J. A. Voigt and B. E. Gnade, *J. Appl. Phys.*, 1996, **79**, 7983.
37 M. L. Kahn, T. Cardinal, B. Bousquet, M. Monge, V. Jubera and B. Chaudret, *ChemPhysChem*, 2006, **7**, 2392.
38 P. A. C. Quist, W. J. E. Beek, M. M. Wienk, R. A. J. Janssen, T. J. Savenije and L. D. A. Siebbeles, *J. Phys. Chem. B*, 2006, **110**, 10315.
39 H. Wang, C. Xie and D. Zeng, *J. Cryst. Growth*, 2005, **277**, 372.
40 H. Lee, W. Jakubowski, K. Matyjaszewski, S. Yu and S. S. Sheiko, *Macromolecules*, 2006, **39**, 4983.
41 R. Xie, D. Li, H. Zhang, D. Yang, M. Jiang, T. Sekiguchi, B. Liu and Y. Bando, *J. Phys. Chem. B*, 2006, **110**, 19147.
42 W. Jia, X. Chen, H. Lu and P. Yang, *Angew. Chem., Int. Ed.*, 2006, **45**, 3345.

